Highlight Review

Localization of Electromagnetic Wave in 3D Periodic and Fractal Structures

Yoshinari Miyamoto, Soshu Kirihara, and Mitsuo Wada Takeda

(Received December 12, 2005; CL-058014)

Abstract

Localization or confinement of electromagnetic or optical waves is reviewed briefly in respect to the wave interaction with the specific structures of periodic, random, and fractal (self-similar) geometries, which can enhance strong interference, scattering, and resonance of waves. The localization of microwave in photonic crystals with diamond structure and in photonic fractals with Menger sponge structure of dielectric media is reported and discussed about the difference of localization behaviors. These 3D structures are fabricated easily from liquid photosensitive resins or ceramic dispersed ones by a CAD/CAM stereolithography. The localization in photonic fractals is supported with several measurements of transmission, 90° wave scattering, electric field intensity profile, and FDTD (finite-difference time-domain) simulation for localized modes. An empirical equation to predict the localization frequencies shows good agreements with measured results as well. The localization in a photonic crystal can be explained by Bragg scattering, while that in a photonic fractal by resonance in the fractal cavity.

♦ Introduction

Localization or confinement of electromagnetic or optical waves in a limited space is an emergent topic in the interdisciplinary area of physics, chemistry, electronics, materials science, and engineering. By localizing these electromagnetic waves a wide range of devices are possible for communication, information, optical, and sensing applications. It is necessary to design particular structures with effective media in order to localize electromagnetic waves. One is the periodic structure of dielectric or metal media which is called photonic crystal.[1–3] It can totally reflect electromagnetic waves with the wavelength similar to the periodicity due to Bragg scattering and form photonic bandgap. In the ban dgap, the wave propagation is inhibited because the plane running wave mode vanishes and changes to the standing wave mode due to the interference of incident and reflected waves with periodic lattices. When a small cavity is formed in a photonic crystal like a lattice defect, the waves in a band gap can be localized or confined with surrounding reflective lattice planes. The reported highest Q factor of the localized mode of light reaches 10^5–10^6 in a 2D photonic crystal slab of Si.[4]

Another possible structure of localization is a randomly distributed structure of scattering media which can induce Anderson localization.[5] When the light is randomly scattered in a disordered structure and the mean free path of running waves is reduced below the wavelength due to multiple interferences, the wave is strongly localized. Such localization is reported in nanosized GaAs[5] and ZnO[6] powders. The concepts of the photonic band gap and the Anderson localization of photons have been derived by analogies of the electronic band gap in semiconductors and the Anderson localization of electrons in disordered systems,[7] respectively. These localizations can be considered as a consequence of the strong interference of light in periodically ordered or disordered structures of scattering media.

Fractal has different geometric structures from periodic ones. The fractal pattern or structure is characterized with the self-similarity.[8] The periodic structure has the translational symmetry that is invariant for translational operation, while the fractal structure has the dilatation symmetry that is invariant for reduction and expansion operation.[9] The wave interaction with fractal structures or patterns shows various interesting behaviors in macro, micro, and nanometer scales. Plane running waves are not eigenfunctions of the operator of dilatation symmetry, so that the incident waves with the specific wavelength associated with the fractal geometry decay or attenuate exponentially. It is thought that complex coastlines may be formed because of the natural optimization of fractal geometry in macro scale, which are self-stabilized against erosion by damping running waves of seawater.[10]

The microwave transmission and reflection to a planar Cu fractal pattern of connected H-shaped lines with fractal dimension 2 on a dielectric plate show various strange behaviors, such as log periodicity of alternate repeating near-total transmissions and reflections as a function of frequency, even though their wavelengths are much larger than the sample size.[11,12] Such log periodicity is an inherent consequence of the self-similarity of fractal patterns. These behaviors are thought due to the local resonances by induced current at any levels of substructures in the H-shaped fractal pattern of Cu.

The strong localization of laser light irradiated to colloidal aggregates of nanosized Ag metal particles with the random fractal structure of fractal dimension $\approx$1.8 is enhanced at local regions smaller than the wavelength, where the electromagnetic energy is concentrated leading to the huge enhancement of resonant Rayleigh, Raman, and nonlinear light scattering.[13,14] Such fractal structure results in localization of plasmon excitations where the local field can exceed the applied field by several orders of magnitude. The localization of light in random fractal

Prof. Yoshinari Miyamoto and Assoc. Prof. Soshu Kirihara
Smart Processing Research Center, Joining and Welding Research Institute,
Osaka University, Mihogaoka 11-1, Ibaraki 567-0047
E-mail: miyamoto@jwri.osaka-u.ac.jp, kirihara@jwri.osaka-u.ac.jp
Prof. Mitsuo Wada Takeda
Department of Physics, Faculty of Science, Shinshu University, Matsumoto 390-8621

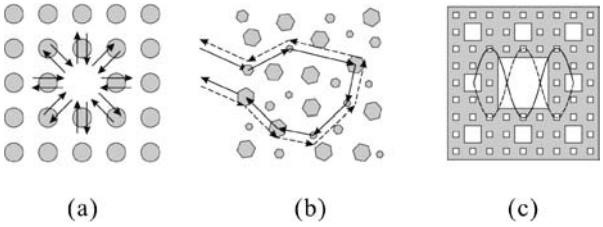

Figure 1. Schematic diagrams showing localizations of electromagnetic wave or light in (a) periodic, (b) random, and (c) fractal structures.

structures and the Anderson localization may be attributed to the similar origin.

Localization of electromagnetic waves or energy at a local space is excited in particular structures with the periodic, disordered, or fractal geometries which can enhance interference, scattering, and/or resonance of waves. These different localizations of electromagnetic wave or light are schematically illustrated in Figure 1.

♦ *Design and Fabrication of 3D Structures for Electromagnetic Wave Localization*

Complex 3D periodic and fractal structures can be designed and fabricated easily by stereolithography of a CAD/CAM system.[15] Stereolithography is used in modern industries to form prototypes of resin and develop optimum design of components in electric goods, cars, machines, and other products. A model structure is sliced into thin sections on a computer and transferred to a stereolithographic machine. This machine forms a 3D object layer-by-layer by scanning a UV laser beam over a liquid photopolymer resin. Figure 2 shows a schematic illustration of a typical stereolithographic machine. We use stereolithography to fabricate not only external shapes, but internal structures like diamond lattices. Fine ceramic particles are dispersed into the liquid resin in order to increase the dielectric constant of photonic crystals and fractals. It is possible to sinter them by burning out resin and successive heating at high temperatures.[16]

♦ *Localization in Diamond Structure*

Diamond structure of dielectric medium is an ideal photonic crystal because it can open the band gap in all directions.[17] Figure 3 shows a CAD image of diamond structure including

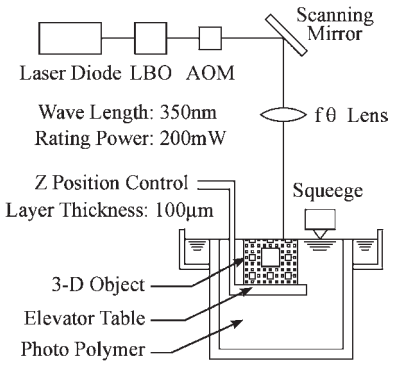

Figure 2. A schematic diagram of stereolithographic machine.

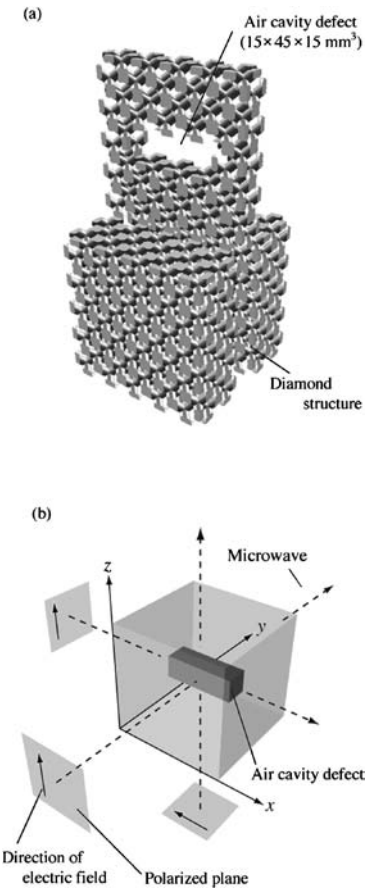

Figure 3. (a) A CAD image of diamond structure containing an air-cavity defect. (b) Schematic diagram of the relationship between microwave direction and air-cavity defect.

an air cavity defect.[18] The diamond lattice without defect consists of $5 \times 5 \times 5$ unit cells with the cell dimension of 15 mm which is composed of 10 vol % TiO_2–SiO_2 dispersed epoxy. Figure 4 shows lower and upper band edges of the photonic band gap in Γ-$L\langle 111\rangle$, Γ-$X\langle 100\rangle$, and Γ-$K\langle 110\rangle$ directions as a function of frequency, that was measured against the incident plane wave of TE_{10} mode by using a network analyzer and a metal cavity. It showed a perfect band gap between 14.3 and

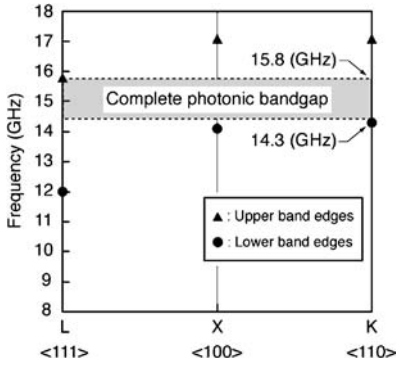

Figure 4. Upper and lower band edges of measured photonic bandgap along Γ-$L\langle 111\rangle$, Γ-$X\langle 100\rangle$, and Γ-$K\langle 110\rangle$ directions. Complete photonic bandgap was observed between 14.3 and 15.8 GHz frequency range.

Published on the web (Advance View) March 11, 2006; DOI 10.1246/cl.2006.342

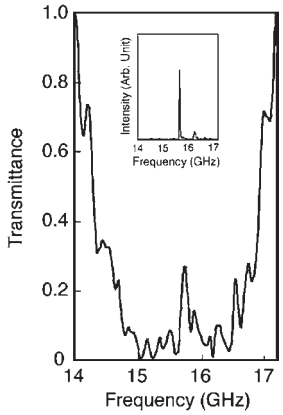

Figure 5. Frequency dependence of the transmission amplitude through diamond structure with the defect along *y* direction. A spectrum of the resonant mode after normalizing with that of defect-free diamond structure is shown in the inset.

15.8 GHz. The calculated band gap by plane wave expansion method[19] confirmed the complete band gap range. Figure 5 shows that a defect mode appears along equivalent directions of *y* and *z* in the band gap when microwaves were radiated normal to the wide sides ($45 \times 15\ mm^2$) of the rectangular shape defect. The Q factor of the localized mode is 300. It is necessary for high Q factor to control scattering of the localized mode three dimensionally besides reducing the dielectric loss of the lattice medium. No such mode appears along the *x* direction in the measured frequency range because of the spatial symmetry of the rectangular shape air cavity. The mode analysis showed the penetration of the electric field or localized wave in an air cavity about 0.16 of the lattice constant in the host photonic crystal.

♦ *Localization in Menger Sponge Structure*

We have fabricated 3D fractal structures called Menger sponge with epoxy or ceramic dispersed epoxy and found that the incident microwave with the specific wavelength was localized in the structure.[20,21] Because no such fractal was known which can localize electromagnetic waves three dimensionally, it was named as photonic fractal. Menger sponge is designed by dividing the initial cube into $3 \times 3 \times 3$ smaller cube pieces and extracting seven pieces at the body and face-centers. When this dividing and extracting operation is repeated three times, a stage 3 Menger sponge is formed as shown in Figure 6.

The fractal dimension *D* is used as a measure to describe the complexity of fractal structures, which is calculated by the following equation:

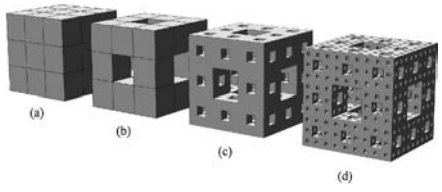

Figure 6. Schematic diagram of Menger sponge structures. (a) Initiator, (b) stage 1 (generator), (c) stage 2, and (d) stage 3.

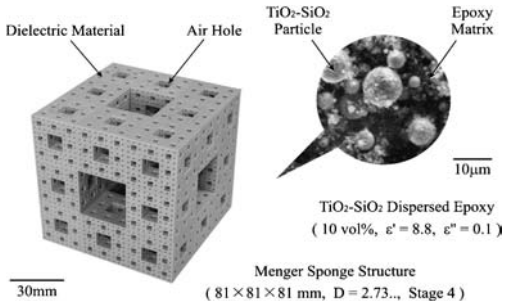

Figure 7. A photo of a stage 4 Menger sponge structure with 10 vol % TiO_2–SiO_2/epoxy with 81 mm cube fabricated by stereolithography.

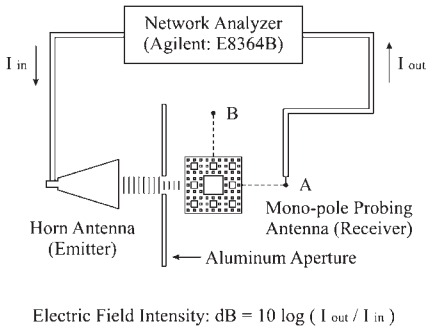

Figure 8. Experimental set up to measure the transmission and the 90° scattering spectra for a stage 4 Menger sponge structure of 10 vol % TiO_2–SiO_2/epoxy with 81 mm cube.

$$N = S^D, \tag{1}$$

where *N* is the number of the self-similar units newly created when the size of the initial unit decreases to $1/S$. In Menger sponge, $N = 20$, and $S = 3$, so that $D = \log 20/\log 3 \cong 2.73$.

Figure 7 shows a stage 4 Menger sponge structure with an edge length of 81 mm, which was formed of 10 vol %TiO_2–SiO_2 dispersed epoxy (measured dielectric constant: 8.8). We measured the transmission spectrum against normally incident plane waves with TE_{10} mode into the central air cavity with 27 mm square of the Menger sponge sample as illustrated in Figure 8. The measurement was performed in a free space using a network analyzer. The microwave was emitted from a horn antenna and detected at position A by using a monopole antenna. An aluminum aperture plate with a 22 mm square window was placed in between a horn antenna and a sample in order to prevent the reflection of wave from the front face of Menger sponge. As seen in Figure 9, a sharp attenuation of transmission amplitude down to −30 dB was observed at 13.5 GHz suggesting the localization in the structure. The wavelength of this mode is 22.2 mm in free space. However, such a transmission spectrum is not enough to ensure the localization because the incident wave may be scattered strongly to other directions.

The FDTD (finite-difference time-domain) simulation of localized modes for the dipole radiation from the outside to the Menger sponge revealed that the measurement of the 90° wave scattering is more reliable rather than that of straight transmission.[22,23] Because the 90° wave scattering is not affected with the incident wave and the spectrum is background free though the electric field intensity is weak. Therefore, we measured

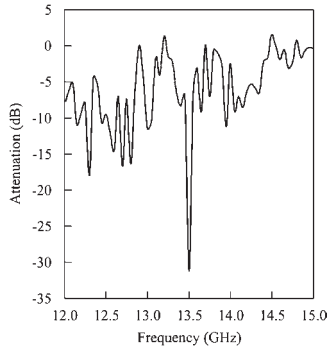

Figure 9. A spectrum of the transmission amplitude measured at position A after normalizing with that of air space without sample.

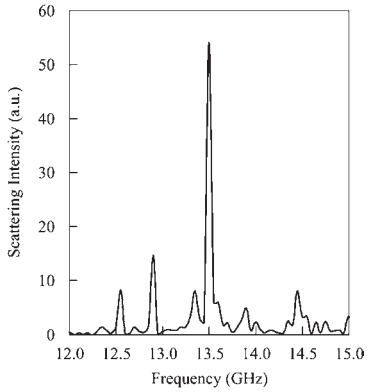

Figure 10. A spectrum of the 90° scattering spectrum measured at position B after normalizing with that of air space without sample.

90° wave scattering at position B using a monopole antenna as illustrated in Figure 8. A relatively strong peak was observed at the same frequency of 13.5 GHz as shown in Figure 10. This spectrum looks similar to the localized peak in the band gap of photonic crystal as seen in Figure 5. However, the 90° wave scattering has no band gap. Therefore, the localization is not due to Bragg scattering, but is a result of the resonance in the fractal cavity. Because this peak is considered as a scattered intensity of the localized wave to all directions, it is possible to estimate the Q factor of the localization from this peak, that was about 180.

The FDTD simulation showed the appearance of multiple localized modes both in air cavities and in dielectric body of the Menger sponge structure when a radiation source by dipole oscillation was placed in the central air cavity.[24] The highest Q factor was calculated as 840 supposing no dielectric loss of medium with the same dielectric constant as 10 vol %TiO_2–SiO_2 dispersed epoxy. The wavelength of this localized mode in free space corresponds to about half edge length of the Menger sponge structure. It is noted that the electromagnetic wave is confined three dimensionally with such high Q factor in a volume whose size is as small as twice the wavelength. Photonic crystals need at least several lattice planes for the strong localization.

A profile of the electric field intensity at the central cross section on the Menger sponge in an x–y plane is shown in Figure 11. This intensity was measured by moving a monopole antenna in and around the Menger sponge structure. The field intensity was most concentrated in the central air cube.

Similar electric filed profiles were obtained for other cross sectional planes. In the case of the stage 3 Menger sponge, the somewhat weak confinement of electric field profile was observed. While, the electric field leaked out of the stage 2 Menger sponge as seen in Figure 12. These results suggest that the strong localization or confinement in dielectric Menger sponge structures needs the stage number higher than 3.

Though the localization mechanism in Menger sponge fractals is not understood well and the experimental results did not meet completely with the FDTD simulation yet, we have derived an empirical equation to predict the frequency of the localized mode in dielectric Menger sponge as follows.[25]

$$\lambda_{\mathrm{conf}} = 2^{\ell} a \sqrt{\varepsilon_{\mathrm{eff}}} / 3^{2\ell-1} \quad (2)$$

where λ_{conf} is the wavelength of the localized mode in air. ℓ is the order number of the localized modes. The effective dielectric constant $\varepsilon_{\mathrm{eff}}$ is the spatially averaged dielectric constant of Menger sponge structure. The filling factor f is the volumetric ratio of remaining parts in an n-dimensional fractal. In the case of stage m Menger sponge, it is expressed by $f = (N/S^n)^m$, where the geometry of fractal is introduced. The effective dielectric constant $\varepsilon_{\mathrm{eff}}$ is given by an equation of a simple mixing rule, $\varepsilon_{\mathrm{eff}} = f\varepsilon_{\mathrm{A}} + (1-f)\varepsilon_{\mathrm{B}}$, where ε_{A} and ε_{B} are dielectric constants of remaining and extracted parts, respectively. The dielectric constant of the bulk epoxy including 10 vol %TiO_2–SiO_2 measured was $\varepsilon_{\mathrm{A}} = 8.8$. $\varepsilon_{\mathrm{B}} = 1$(air).

Table 1 compares the calculated and measured frequencies of localization in the Menger sponge samples with different sizes, stages, and dielectric constants. In smaller Menger sponges (27 mm cube) of epoxy and TiO_2–SiO_2/epoxy which were measured in a metal cavity, the localized frequencies at 12.8 and 8.0 GHz, respectively, show good agreements with the calculated ones as the first localized mode ($\ell = 1$). The calculated frequencies for the second modes ($\ell = 2$) were 57.5 and 36.6 GHz, respectively. These frequencies were too high and out of measurable range in our measurement system.

For the stage 3 and 4 Menger sponges (81 mm cube), the measured frequencies were 12.0 and 13.6 GHz, respectively. These values agree well with the calculated ones for the second modes. The calculated frequencies for the first modes were low and out of measurable range. Though the physical meaning of the empirical equation is not defined yet, it may give a simple model of localization that the first mode resonates with 1.5 wavelength in a space of Menger sponge structure.

Table 1. Measured and calculated frequencies of localized modes in various Manger sponge structures

Cube Size; a /mm	Stage Number; m	Effective Dielectric Constant; $\varepsilon_{\mathrm{eff}}$	Calculated Localized Frequency ($\ell = 1$) /GHz	Calculated Localized Frequency ($\ell = 2$) /GHz	Measured Localized Frequency /GHz
27	3	1.7	12.8	57.5	12.8
27	3	4.2	8.1	36.6	8.0
81	3	4.2	2.7	12.2	12.0
81	4	3.3	3.1	13.8	13.6

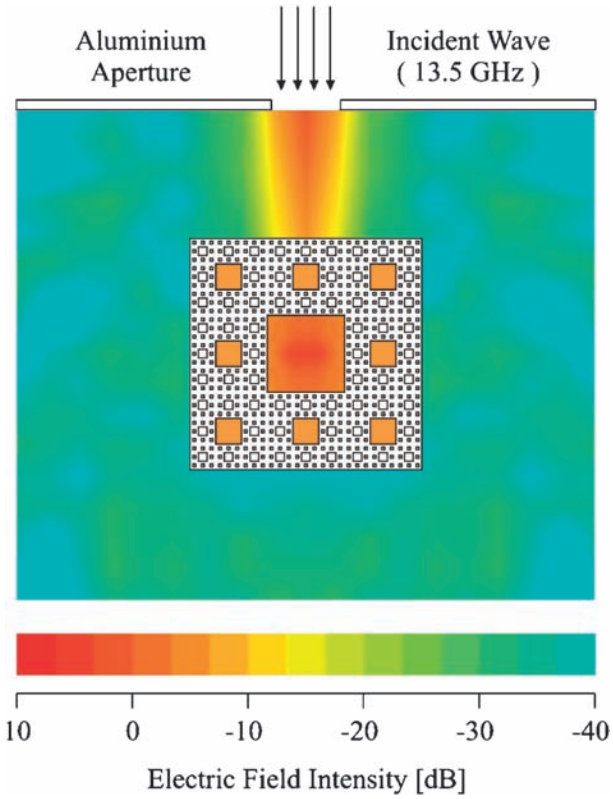

Figure 11. Electric field intensity profile at the inner and outer space of the stage 4 Menger sponge structure.

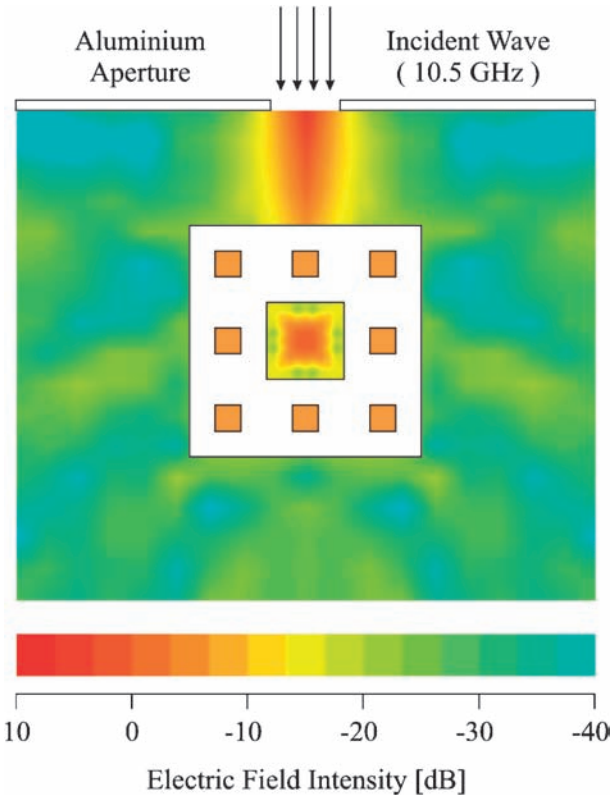

Figure 12. Electric field intensity profile at the inner and outer space of the stage 2 Menger sponge structure.

It is expected to localize terahertz wave or light by fabricating smaller 3D photonic crystals and fractals with micrometer or nanometer sizes. Especially, terahertz wave is paid increasing attention as a virgin light left in between electromagnetic waves and light because of a large potential of application to sensors for surface flaws, cancer of the skin, bacteria in foods, gun powder, drug, etc. besides to high speed and large volume communication systems.[26,27] We are developing miniaturized photonic crystals and fractals with ceramics to produce a compact terahertz wave source and control. These results will be reported elsewhere.

♦ Summary

Localization phenomena of electromagnetic waves have been reviewed associated with our recent study on photonic crystals and fractals. These localization functions are created by particular structures such as periodically ordered, disordered, or fractal geometries rather than materials. The CAD/CAM stereolithography is a useful tool to engineer these structures three dimensionally. The wave interaction with fractal structures is very interesting, however, further experimental and theoretical study is necessary to understand the localization mechanism. The control of electromagnetic wave or light with periodic, fractal, and random structures would open a new photonic science and technology.

The authors appreciate the enlightening discussion on the electromagnetic properties of photonic crystals and fractals with Dr. Kazuaki Sakoda of National Institute for Materials Science, Prof. Katsuya Honda of Shinshu University, and Dr. Shingo Kanehira of Kyoto University. This work is supported by the Grant for the 21st Century COE Program "Center of Excellence for Advanced Structural and Functional Materials Design," and by the Grant-in-Aid for Scientific Research (S) No. 171067010, both under the auspice of the Ministry of Education, Culture, Sports, Science and Technology, Japan.

References

1 E. Yablonovitch, *J. Mod. Opt.* **1994**, *41*, 173.
2 J. D. Joannopoulos, R. D. Maeda, J. N. W. Sinn, *Photonic Crystals*, Princeton University Press, **1995**.
3 *Photonic Crystals, Physics, Fabrication and Applications*, ed. by K. Inoue, K. Ohtaka, Springer, **2004**.
4 Y. Akahane, T. Asano, B. S. Song, S. Noda, *Opt. Express* **2005**, *13*, 1202.
5 D. S. Wiesma, P. Bartolini, A. Lagendijk, R. Righini, *Nature* **1997**, *390*, 671.
6 H. Cao, Y. G. Zhao, S. T. Ho, E. W. Seeling, Q. H. Wang, R. P. H. Chang, *Phys. Rev. Lett.* **1999**, *82*, 2278.
7 P. W. Anderson, *Phys. Rev.* **1958**, *109*, 1492.
8 B. B. Mandelbrot, *The Fractal Geometry of Nature*, W. H. Freeman & Company, San Fransisco, **1982**.
9 X. Sun, D. L. Jaggard, *J. Appl. Phys.* **1991**, *70*, 2500.
10 B. Sapoval, Th. Gobron, A. Margolina, *Phys. Rev. Lett.* **1991**, *67*, 2974.
11 W. Wen, L. Zhou, J. Li, W. Ge, C. T. Chan, P. Sheng, *Phys. Rev. Lett.* **2002**, *89*, 223901.
12 L. Zhou, W. Wen, C. T. Chan, P. Sheng, *Appl. Phys. Lett.* **2003**, *82*, 1012.

13 V. A. Markel, V. M. Shalaef, E. B. Stechel, W. Kim, R. L. Armstrong, *Phys. Rev.* **1996**, *53*, 2425.
14 V. M. Shalaef, *Topics in Applied Physics*, Springer-Verlag Berlin Heidelberg, **2002**, Vol. 82, p. 93.
15 S. Kirihara, Y. Miyamoto, K. Takenaga, M. W. Takeda, K. Kajiyama, *Solid State Commun.* **2002**, *121*, 435.
16 S. Kanehira, S. Kirihara, Y. Miyamoto, *J. Am. Ceram. Soc.* **2005**, *88*, 1461.
17 J. W. Haus, *J. Mod. Opt.* **1994**, *41*, 195.
18 S. Kanehira, S. Kirihara, Y. Miyamoto, K. Sakoda, M. W. Takeda, *J. Am. Ceram. Soc.* **2005**, *88*, 2480.
19 K. M. Ho, C. T. Chan, C. M. Soukoulis, *Phys. Rev. Lett.* **1990**, *65*, 3152.
20 M. W. Wada, S. Kirihara, Y. Miyamoto, K. Sakoda, K. Honda, *Phys. Rev. Lett.* **2004**, *92*, 093902.
21 Y. Miyamoto, S. Kirihara, S. Kanehira, M. W. Takeda, K. Honda, K. Sakoda, *Int. J. Appl. Ceram. Technol.* **2004**, *1*, 40.
22 K. Sakoda, S. Kirihara, Y. Miyamoto, M. W. Takeda, K. Honda, *Appl. Phys. B* **2005**, *81*, 321.
23 K. Sakoda, *Opt. Express* **2005**, *13*, 9585.
24 K. Sakoda, *Phys. Rev. B* **2005**, *72*, 184201.
25 Y. Miyamoto, S. Kirihara, M. W. Takeda, K. Honda, K. Sakoda, The 29th International Conference on Advanced Ceramics and Composites, The American Ceramic Society, **2005**, p. 349.
26 D. R. Dykaar, S. L. Chuang, *J. Opt. Soc. Am. B* **1994**, *11*, 2454.
27 M. Iida, M. Tani, K. Sakai, M. Watanabe, S. Katayama, H. Kondo, H. Kitahara, S. Kato, M. W. Takeda, *Phys. Rev. B* **2004**, *69*, 245119.